Wide fluctuations in fluorescence lifetimes of individual rovibronic levels in SiH2 (Ã1 B 1)

J. W. Thoman Jr., J. I. Steinfeld, R. I. McKay, and A. E. W. Knight

Citation: The Journal of Chemical Physics **86**, 5909 (1987); doi: 10.1063/1.452475
View online: http://dx.doi.org/10.1063/1.452475
View Table of Contents: http://scitation.aip.org/content/aip/journal/jcp/86/11?ver=pdfcov
Published by the AIP Publishing

Wide fluctuations in fluorescence lifetimes of individual rovibronic levels in SiH_2 ($\tilde{A}\,^1B_1$)

J. W. Thoman, Jr. and J. I. Steinfeld
Department of Chemistry, Massachusetts Institute of Technology, Cambridge, Massachusetts 02139
R. I. McKay and A. E. W. Knight
School of Science, Griffith University, Nathan, Brisbane, Queensland 4111, Australia

(Received 18 November 1986; accepted 20 February 1987)

We have measured fluorescence lifetimes of individual rovibronic levels in SiH_2 ($\tilde{A}\,^1B_1$, 020). The lifetimes vary widely from one level to the next, ranging from $\lesssim 10$ ns to $> 1\,\mu$s. Similar behavior is seen in the (000), (010), and (030) levels. This behavior is interpreted in terms of coupling of the $\tilde{A}\,^1B_1$ rovibronic levels with background levels in the $\tilde{X}\,^1A_1$ (S_0) and $\tilde{a}\,^3B_1$ (T_1) states, and thence via predissociation to $Si(^3P) + H_2$. The irregular variation in the lifetimes reflects the quasirandom spacings of S_0 and T_1 levels in the vicinity of any particular $\tilde{A}$ state level.

I. INTRODUCTION

Silylene (SiH_2) has been identified as a key intermediate in the decomposition of silicon hydrides, such as the chemical vapor deposition of amorphous silicon (*a*:Si–H) from monosilane[1] or higher silanes,[2] and in the pyrolysis of silane.[3] Infrared excitation of suitable precursors also leads to production of SiH_2. While direct infrared multiple-photon dissociation (IRMPD) of SiH_4 itself cannot be accomplished under collision-free conditions[4] this species can undergo sensitized decomposition in the presence of SiF_4,[5] while substituted organosilanes $RSiH_3$ (R = ethyl, *n*-butyl, or phenyl) undergo facile IRMPD.[6]

The formation of SiH_2 in IRMPD of organosilanes has been established by its detection using laser-excited fluorescence (LIF)[7,8] in the $\tilde{A}\,^1B_1 \leftrightarrow \tilde{X}\,^1A_1$ band. This intermediate has also been detected following UV photolysis of phenylsilane.[9] During our initial investigations of this species,[7] we noticed that the fluorescence excitation intensity distribution within a vibrational band varied markedly with the detector gate setting, indicating a wide dispersion in fluorescence lifetimes for different rotational levels in the excited state. We have carried out additional experiments on the IRMPD of organosilanes, and have measured fluorescence lifetimes for a large number of resolved rovibronic states in the (000), (010), (020), and (030) vibrational levels of $\tilde{A}\,^1B_1$ SiH_2. Rotational assignments are available for the $\tilde{A}(020)$–$\tilde{X}(000)$ band,[10] but many transitions remain unassigned. In this paper we report lifetimes of ~ 220 rovibronic states accessed via transitions in the $\tilde{A}(020)$–$\tilde{X}(000)$ band. Of these, ~ 100 states are identified from known rotational assignments. A model is presented which accounts for the wide spread of observed lifetimes ($\lesssim 10$ ns to $\sim 1\,\mu$s) and which offers insight on the likely nature of S_1–S_0 and S_1–T_1 interactions in SiH_2.

II. EXPERIMENTAL DETAILS

SiH_2 was produced by IRMPD of *n*-butylsilane (Silar Industries) which was slowly flowed through the experimental chamber at a pressure of 5 mTorr or less. A CO_2 TEA laser (Laser Science PRF-150s) provided pulses with a fluence of 5 J/cm^2 at the 10*P*(20) line (944 cm^{-1}) and a repetition rate of 20 Hz. Single rotational levels in the $\tilde{A}\,^1B_1(020) \leftarrow \tilde{X}\,^1A_1(000)$ vibronic band were excited by 100 μJ, 10 ns, 0.5 cm^{-1} FWHM pulses from an excimer-pumped dye laser (Lambda Physik EMG101E + FL2002). The resulting LIF was imaged through a Corning 2-62 glass filter onto a Hamamatsu R928 photomultiplier with a rise time of 2.2 ns. The overall equipment-limited time constant is approximately 5 ns. The delay between photolysis and LIF probe laser pulses was kept at 2 μs or less for most of the experiments. Other details have been described elsewhere.[7]

Excitation spectra were collected with a gated integrator and boxcar averager (EG&G/PAR 162/165) and displayed on a strip-chart recorder. Fluorescence decay curves of individual rotational levels were collected with a Tektronix 7912AD transient digitizer controlled by a MINC-11/03 laboratory computer. Typically 1024 laser shots were averaged to produce one decay curve. Background scans, produced by blocking the probe laser, were collected for each decay curve and subtracted from that curve to give a zero base line. The data records were transmitted to a VAX computer for analysis of the observed decay curves in terms of single or double exponentials, using a least-squares method.

The production of SiH_2 via UV photolysis of phenylsilane (Silar Industries) was also investigated. As with the IR photolyses, collinear and counterpropagating loosely focused photolysis and probe laser beams were employed. An excimer laser (Lumonics 860-1) provided 1 to 5 mJ per pulse in a 10 ns FWHM pulse at either 193 nm (ArF) or 248 nm (KrF). In additional experiments at Griffith University, UV pulses were generated using the frequency quadrupled output of a Molectron Nd:YAG laser system in conjunction with a 0.5 m Raman cell filled with H_2. The fourth harmonic of the Nd:YAG at 266 nm, and the first three anti-Stokes lines were used for photolysis, along with a Molectron dye laser pumped by a second Nd:YAG laser for the probe. An EMI 9816QB photomultiplier tube was used for detection in the latter experiments.

 0021-9606/87/115909-09$02.10

III. RESULTS

A. SiH_2 production mechanisms

The most efficient method we have found for production of SiH_2 is IRMPD of alkylsilanes, such as *n*-butylsilane. Two mechanisms have been proposed for this dissociation, a four-center elimination of silane,[6]

$$CH_3CH_2CH_2CH_2SiH_3 \rightarrow CH_3CH_2CH{=}CH_2 + SiH_4 \quad (I)$$

and a three-center elimination of H_2,[8]

$$CH_3CH_2CH_2CH_2SiH_3 \rightarrow CH_3CH_2CH_2CH_2SiH + H_2. \quad (II)$$

In these mechanisms, the SiH_2 is not a primary photolysis product, but rather arises from secondary IRMPD either of the vibrationally "hot" silane produced in (I), or of the substituted silylene in (II). The experiments reported here cannot distinguish between these two possibilities; the SiH_2 signal is observed within the CO_2 laser pulse, indicating rapid secondary IRMPD. A third possible mechanism, three-center elimination to produce SiH_2 directly,

$$CH_3CH_2CH_2CH_2SiH_3 \rightarrow C_4H_{10} + SiH_2 \quad (III)$$

was discounted on the basis of the low yield observed of saturated alkane.[6]

Molecular orbital calculations at the 3-21G level in the analogous ethylsilane system[11] suggest that while the mechanism (I) products are thermodynamically most stable, the four-center elimination channel required to reach them has the highest potential energy barrier. The lowest barrier is associated with the least stable products, i.e., mechanism (II). Additional evidence for mechanism (II) is that while the calculated barriers for (I) and (III) lie above the SiH_2^* ($\tilde{A}\,^1B_1$) excitation energy, no spontaneous chemiluminescence is observed. Additional calculations on the RRKM rates for each of these dissociation channels are currently in progress.[11]

Although SiH_2 has been frequently observed in the UV photolysis of phenylsilane,[7-9,12] it appears to be formed in much lower yield in this case than in the alkysilane IRMPD. Based on comparison of relative LIF signal strengths, photolysis of ϕSiH_3 at 193 nm yields only on the order of 1% as much SiH_2 as does the alkylsilane IRMPD, under our experimental conditions. Use of 248 or 266 nm photolysis wavelengths yields no detectable SiH_2, even though the pulse energies are 5 to 30 times greater than at the 193 nm wavelength. Measurements were also made at wavelengths Raman shifted from the Nd:YAG fourth harmonic, viz., 240 nm (AS_1), 218 nm (AS_2), and 200 nm (AS_3). In none of these instances could SiH_2 be observed. Eley *et al.*[13] have decomposed ϕSiH_3 with the 206 nm output of an iodine lamp, presumably with intermediate formation of SiH_2. These experiments measured integrated product yield, however, and a quantum yield was not established. Our failure to observe SiH_2 with photolysis at 200 nm is probably due to the extremely low pulse energy available to us at that wavelength. It may also be noted that IRMPD of ϕSiH_3 produces SiH_2 at a yield only a few percent of that for butylsilane, under similar conditions,[7] even though ϕSiH_3 undergoes quite facile IRMPD.[6] In summary, it appears that ϕSiH_3 can be photolyzed only in the $^1B_{1u} \leftarrow {}^1A_{1g}$ absorption band below 210 nm, in agreement with the conclusions of Eley *et al.*,[13] and that SiH_2 formation is only a minor channel in the UV or IRMP dissociation of ϕSiH_3. This will be important later for estimating the SiH_2 $\tilde{A}\,^1B_1$–$\tilde{X}\,^1A_1$ transition moment from absorbance data.

B. Lifetime measurements

Decay curves were measured, as described above, following excitation of 220 lines in the (020)–(000) band of the $\tilde{A}\,^1B_1$–$\tilde{X}\,^1A_1$ transition of SiH_2. Of these, about half could be identified with specific rotational levels using the assignments of Dubois.[10] The remaining lines have not been assigned and are probably perturbed, as will be discussed further below. Most of the observed decay curves are exponential, as illustrated by the example shown in Fig. 1(a). Decay times derived from an exponential fit to the data and associated rotational assignments, where known, are given in Table I. The precision of the exponential fit is generally within ± 5%. Ta-

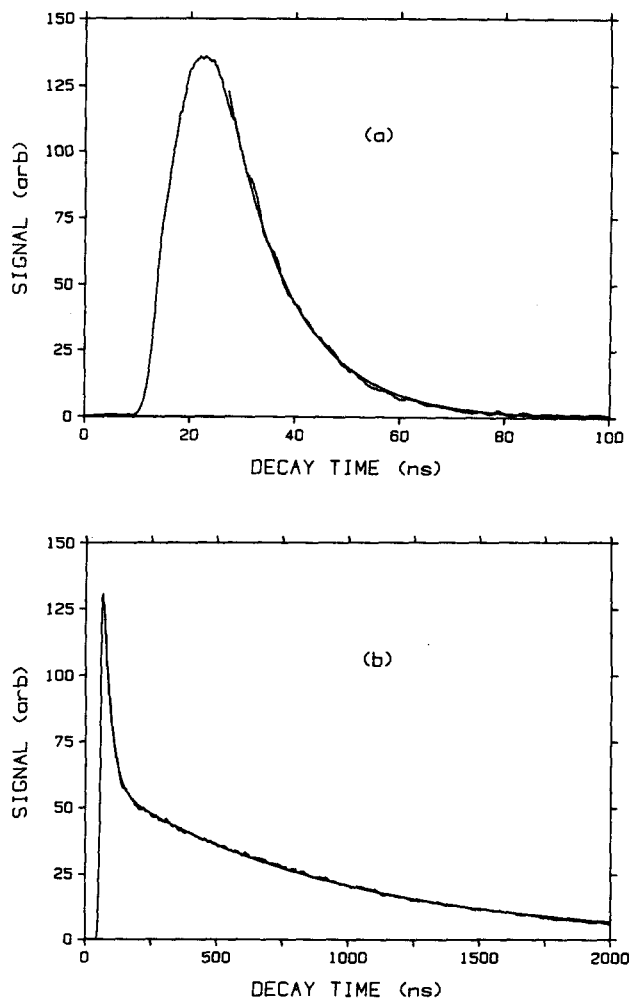

FIG. 1. Measured decay times of selected rovibronic levels in SiH_2 $\tilde{A}\,^1B_1(020)$. (a) 7_{17}–7_{25} line at 17 167.3 cm^{-1}; decay time = 13 ns. (b) Excitation of blended 0_{00}–1_{10} and 1_{10}–2_{20} features at 17 231.9 cm^{-1}; decay times = 27 and 898 ns. We believe that the long decay time should be assigned to the 0_{00} level.

TABLE I. Measured decay times for excitation features in the (020)–(000) band of the $\tilde{A}\,^1B_1$–$\tilde{X}\,^1A_1$ transition in SiH_2.

$\tilde{\nu}$, cm^{-1}	Assignment[a]	τ, ns	$\tilde{\nu}$, cm^{-1}	Assignment[a]	τ, ns	$\tilde{\nu}$, cm^{-1}	Assignment[a]	τ, ns	$\tilde{\nu}$, cm^{-1}	Assignment[a]	τ, ns
17 481.4	$6_{42}-6_{34}$	7	17 342.8		75	17 259.7	$5_{15}-5_{05}+5_{05}-4_{13}$	17	17 202.2	$3_{13}-4_{23}$	12
17 480.8	$6_{33}-5_{05}$	10	17 340.1		14	17 258.6	$3_{03}-2_{11}+4_{04}-3_{12}$	12	17 198.6		7
17 480.8	$6_{33}-5_{05}$	129	17 338.9		9	17 258.1	$6_{16}-6_{06}+7_{17}-7_{07}$	60	17 197.1		122
17 479.1		38	17 334.4		1275	17 257.3		10	17 194.3		8
17 474.2	$8_{44}-7_{52}+9_{46}-8_{54}$	8	17 332.4	$8_{44}-9_{36}+5_{23}-5_{15}$	6	17 254.2	$2_{11}-2_{21}$	137	17 191.6	$3_{12}-4_{22}$	9
17 472.2	$7_{43}-7_{35}$	9	17 330.3	$4_{22}-4_{14}$	5	17 254.2	$2_{11}-2_{21}$	8	17 191.0		22
17 471.8		12	17 329.5		7	17 252.6		30	17 190.0		9
17 460.3		401	17 329.5		126	17 251.1		112	17 190.0		789
17 460.3		6	17 327.4	$3_{31}-4_{41}$	7	17 251.1		8	17 189.1		9
17 457.5		6	17 323.8		6	17 250.3	$8_{17}-8_{27}$	738	17 183.6	$3_{03}-4_{13}+6_{15}-6_{43}$	22
17 444.9		7	17 322.3	$4_{31}-5_{23}+10_{37}-9_{63}$	5	17 250.3	$8_{17}-8_{27}$	11	17 181.8		7
17 444.9		434	17 320.8	$5_{23}-4_{31}+5_{14}-4_{04}$	22	17 249.8		7	17 181.2		991
17 442.1	$9_{28}-8_{18}$	7	17 317.4	$7_{26}-6_{34}$	9	17 249.5	$7_{07}-7_{17}$	106	17 181.2		12
17 439.4		13	17 316.5	$10_{46}-11_{38}$	7	17 249.5	$7_{07}-7_{17}$	28	17 180.3		228
17 431.4	$7_{35}-7_{07}$	104	17 314.8		822	17 248.6		23	17 178.7		133
17 428.9	$4_{31}-3_{21}$	5	17 312.6		6	17 247.8	$6_{06}-6_{16}$	6	17 175.7		10
17 420.9	$6_{33}-5_{23}$	23	17 312.6		612	17 245.6	$5_{05}-5_{15}+5_{14}-5_{24}$	10	17 172.1	$6_{06}-6_{34}$	9
17 415.0	$9_{46}-9_{36}$	31	17 311.7		9	17 244.2	$1_{01}-1_{11}+7_{16}-7_{26}$	121	17 169.3	$4_{04}-5_{14}+5_{15}-6_{25}$	166
17 412.7		80	17 311.7		220	17 243.2	$2_{02}-2_{12}+$ others	19	17 169.3	$4_{04}-5_{14}+5_{15}-6_{25}$	15
17 407.5	$4_{41}-5_{51}$	13	17 311.5		9	17 242.6	$3_{03}-3_{13}$	14	17 168.0	$7_{26}-8_{36}$	8
17 406.4	$4_{40}-5_{50}$	13	17 309.5		7	17 241.7		111	17 167.3	$7_{17}-7_{25}$	13
17 404.5	$3_{30}-3_{22}$	8	17 307.8	$3_{22}-3_{12}$	6	17 241.7		10	17 165.5		9
17 396.1	$4_{31}-4_{23}+3_{31}-3_{21}$	5	17 307.0	$9_{28}-9_{18}$	9	17 241.5	$3_{21}-4_{31}$	11	17 163.6		1175
17 394.6	$6_{33}-5_{41}$	9	17 306.3	$4_{13}-3_{03}$	12	17 241.5	$3_{21}-4_{31}$	122	17 162.7		7
17 393.2		8	17 306.3	$4_{13}-3_{03}$	86	17 240.2		49	17 159.4		81
17 392.4	$7_{26}-6_{16}+5_{32}-5_{24}$	9	17 302.0	$4_{32}-5_{42}$	94	17 238.3		12	17 158.8		6
17 392.4	$7_{26}-6_{16}+5_{32}-5_{24}$	110	17 302.0	$4_{32}-5_{42}$	10	17 237.5		159	17 158.0	$5_{24}-6_{52}$	7
17 388.1	$9_{37}-8_{45}$	10	17 301.1		9	17 235.2		919	17 156.6		22
17 386.3		8	17 297.8	$8_{26}-7_{34}$	20	17 235.2		38	17 155.4	$5_{05}-6_{15}$	7
17 385.2	$7_{35}-6_{43}$	5	17 296.9	$5_{24}-5_{14}$	7	17 233.6	$1_{11}-2_{21}$	17	17 154.2		6
17 383.7		124	17 295.9	$4_{31}-5_{41}$	6	17 231.9	$0_{00}-1_{10}+1_{10}-2_{20}$	27	17 152.6		8
17 383.7		7	17 290.6	$6_{25}-6_{15}$	8	17 231.9	$0_{00}-1_{10}+1_{10}-2_{20}$	898	17 150.2		87
17 381.2	$5_{42}-6_{52}$	11	17 287.7	$7_{26}-7_{16}$	6	17 230.2		9	17 149.9		7
17 379.4		127	17 285.0		8	17 230.2		1082	17 148.3		14
17 377.9	$6_{42}-7_{34}$	7	17 285.0		741	17 225.5		1130	17 146.7		10
17 375.1		13	17 278.9	$9_{19}-9_{09}+4_{13}-3_{21}$	16	17 225.5		8	17 145.2		8
17 371.7	$5_{24}-4_{14}$	9	17 277.3	$1_{10}-0_{00}$	14	17 223.8	$8_{17}-7_{43}$	856	17 141.9		7
17 370.6	$10_{37}-9_{45}$	26	17 273.9	$5_{15}-4_{23}$	8	17 223.8	$8_{17}-7_{43}$	30	17 139.9		29
17 361.7	$4_{23}-3_{13}$	40	17 272.2	$7_{17}-6_{25}$	14	17 222.0	$7_{35}-8_{45}$	58	17 139.3	$6_{15}-7_{25}$	77
17 361.7	$4_{23}-3_{13}$	9	17 271.1		12	17 219.3		8	17 138.0	$7_{17}-8_{27}$	7
17 360.4		207	17 271.1		196	17 220.2	$6_{06}-5_{32}$	7	17 137.4		12
17 359.6	$4_{31}-4_{41}$	5	17 270.1		57	17 217.9	$2_{12}-3_{22}$	7	17 137.0		13
17 358.0	$8_{26}-8_{18}$	20	17 270.1		108	17 217.2		9	17 136.8		10
17 356.8		126	17 268.9		11	17 215.9		10	17 136.3		9
17 356.8		6	17 268.1		10	17 215.5		12	17 135.0		9
17 355.3		473	17 268.1		290	17 213.2	$7_{26}-7_{34}+2_{11}-3_{21}$	12	17 133.9		9
17 355.3		9	17 266.6	$1_{11}-1_{01}$	16	17 212.8		7	17 132.7		24
17 354.5	$6_{34}-6_{24}$	7	17 265.4	$2_{20}-3_{30}$	7	17 211.8		80	17 129.8		11
17 353.5	$7_{43}-8_{35}$	6	17 264.8		72	17 210.5		13	17 126.7		129
17 352.9	$3_{22}-2_{12}$	16	17 264.6		10	17 208.4		31	17 123.0		9
17 348.4		304	17 263.8	$2_{12}-2_{02}+$ others	13	17 207.6	$5_{24}-6_{34}$	678	17 120.6		10
17 347.6		8	17 261.8	$6_{06}-5_{14}+3_{13}-3_{03}$	150	17 207.6	$5_{24}-6_{34}$	61	17 120.3		11
17 346.1		84	17 261.8	$6_{06}-5_{14}+3_{13}-3_{03}$	7	17 205.2		422	17 119.0		397
17 346.1		10	17 261.0	$4_{14}-4_{04}$	9	17 204.9		58	17 117.7		23
17 345.5	$4_{22}-3_{12}+2_{21}-1_{11}$	164	17 259.7	$5_{15}-5_{05}+5_{05}-4_{13}$	109	17 203.8	$8_{36}-9_{46}$	19	17 117.7		107
17 345.5	$4_{22}-3_{12}+2_{21}-1_{11}$	8				17 202.6	$9_{28}-9_{36}$	10			

[a] Following standard spectroscopic notation, upper state rotational quantum numbers are given as $J_{K_aK_c}$, with upper state quantum numbers given first. Assignments are based on those of Dubois (Ref. 10). For the (020) band, $\tilde{\nu}_0 = 17\,248.2\ cm^{-1}$, $A = 24.80\ cm^{-1}$, $B = 5.23\ cm^{-1}$, $C = 3.91\ cm^{-1}$.

ble I also includes lifetimes derived from a number of measurements in which nonexponential decay curves were observed. These nonexponential decays were analyzed readily in terms of a sum of two exponentials, as shown in Fig. 1(b). The most obvious explanation for biexponential (or multiexponential) decay in these instances is that two (or more) different transitions were simultaneously excited, due to blending of some rotational lines in the SiH_2 $\tilde{A}$–$\tilde{X}$ transition. Interpretation in terms of intermediate-case behavior is unlikely to be correct, as discussed further below.

We contrast our observations of a few biexponential decays among mainly exponential decays, with the observations of Inoue and Suzuki.[14] These authors used broader bandwidth excitation and noted that most of their observed fluorescence decays were double exponential, with a "weak, fast component" of 30–60 ns, and a "main, slow component" of 0.6 μs. Such an apparently biexponential decay can arise from a superposition of fluorescence signals from levels with a wide range of decay rates,[15,16] which would be excited with the relatively broadband excitation used by Inoue and Suzuki in

their measurements.

The most striking aspect of our data is the very wide variation in measured lifetimes, from only a few ns—near the lower limit of the response time of the measuring apparatus—to greater than 1 μs. Since, under our conditions, the mean free time between gas-kinetic collisions is $> 10\,\mu$s, all but the very longest lifetimes should be unaffected by collisional quenching.

Figure 2 shows the distribution of our measured lifetimes just for those transitions which have been assigned, ordered by rotational energy in the upper vibronic level. Most of the lifetimes for these transitions are 150 ns or less, with only a few of the very long lifetimes appearing. Figure 3 illustrates the scatter observed in all of the measured lifetimes. Here the lifetimes are sorted by excitation line position rather than by $\tilde{A}\,^1B_1$ (020) rotational energy simply because assignments are unknown for about half the decaying levels. Nevertheless, these data illustrate further that the spread in lifetimes is substantial.

Lifetimes measured following excitation of lines in the (000), (010), and (030) bands of the SiH_2 $\tilde{A}$–$\tilde{X}$ transition also display a wide variation, from a few ns to $\sim 1.5\,\mu$s, but as for the (020) level, the majority of lifetimes are observed to lie within the range $\lesssim$ 10–150 ns. Figure 4 illustrates this qualitatively by way of excitation spectra of the (000)–(000) band, measured as a function of detector gate delay after the fluorescence excitation pulse. In each case, the SiH_2 population sampled is the nascent ground-state distribution after the photolysis pulse. The uppermost spectrum corresponds to fluorescence detection in the time range 0–50 ns, following the excitation pulse. The next two spectra correspond to detection time ranges 185–235 ns and 835–885 ns, respectively. Inspection of the rotational lines marked "*x*", "*y*", and "*z*" shows that there is a dramatic variation in the persistence of fluorescence from the three $\tilde{A}\,^1B_1$ (000) rotational states responsible for these features. The feature labeled *x* corresponds to a relatively short-lived $^1B_1$ state. Although it is the brightest line in Fig. 4(a) (0–50 ns), feature *x* has almost vanished in Fig. 4(c) (835–885 ns). In contrast, feature *z* persists with appreciable intensity, even at the longest delay times. Feature *y* provides an example of an emitting state with an intermediate lifetime.

We are confident that the long fluorescence decay times are in fact attributable to SiH_2 rather than to an impurity. A concern that we have addressed is whether the methylene radical may be responsible for some or all of the observed long decays. It is conceivable that photolysis of butylsilane could lead to some CH_2 ($\tilde{a}\,^1A_1$) fragments; the $\tilde{b}\,^1B_1 \leftarrow \tilde{a}\,^1A_1$ transition of CH_2 overlaps the spectral region occupied by the SiH_2 $\tilde{A} \leftarrow \tilde{X}$ transition; fluorescence lifetimes of levels in the CH_2 $\tilde{b}\,^1B_1$ state are in the microsecond range.

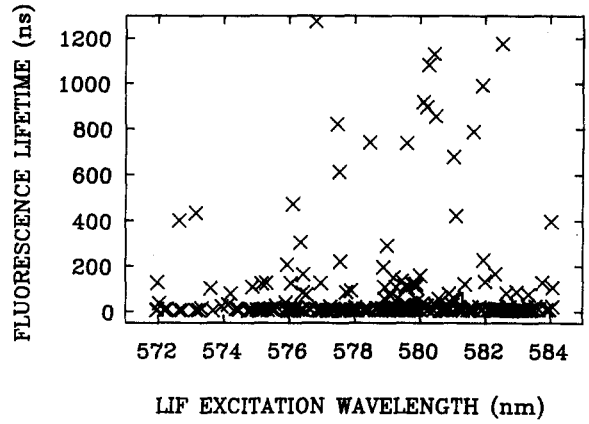

FIG. 3. Measured fluorescence decay times for all observed features in the SiH_2 $\tilde{A}\,^1B_1(020) \rightarrow \tilde{X}\,^1A_1(000)$ band, ordered by excitation wavelength.

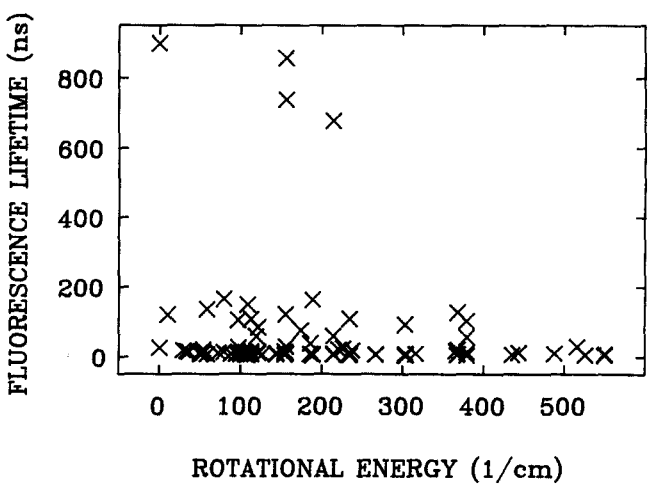

FIG. 2. Fluorescence lifetimes for assigned transitions in the $\tilde{A}\,^1B_1(020)$–$\tilde{X}\,^1A_1(000)$ band of SiH_2, ordered by rotational energy in the excited (020) state.

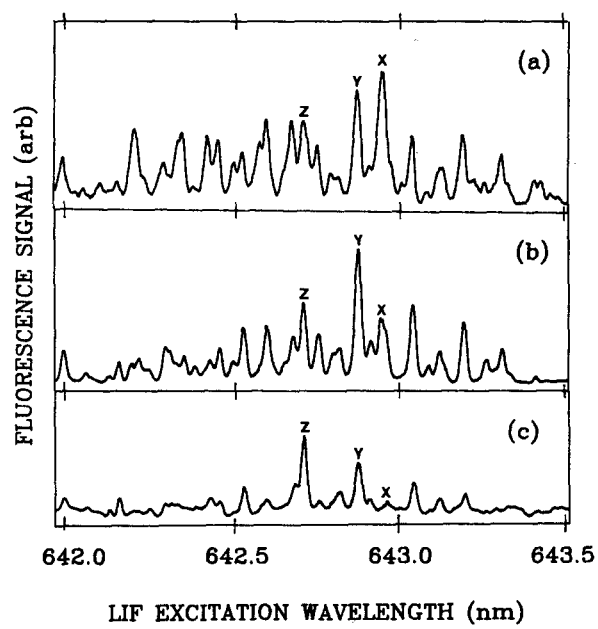

FIG. 4. Fluorescence excitation spectrum of a portion of the SiH_2 $\tilde{A}\,^1B_1(000)$–$\tilde{X}\,^1A_1(000)$ band at detection gate settings (a) 0–50 ns, (b) 185–235 ns, (c) 835–885 ns after the excitation pulse. Spectra are normalized to the peak marked *z*. See the text for discussion of marked features.

However, a careful examination of the known line positions for the CH_2 $\tilde{b}\leftarrow\tilde{a}$ transition[17] reveals that none of the observed features in the SiH_2 $\tilde{A}(020)$–$\tilde{X}(000)$ band correspond to known CH_2 transitions. The SiH $A\,^2\Delta\leftrightarrow X\,^2\Pi$ band is in the 410 nm region.[18] SiH_3 is not expected to be a photolysis product, and in any case its absorption, and those of other species expected to be present (SiH_4, hydrocarbons, etc.), all lie in the UV.

IV. DEVELOPMENT OF A THEORETICAL MODEL

The wide variation in fluorescence lifetimes found for the SiH_2 $\tilde{A}\rightarrow\tilde{X}$ transition would appear to be an extreme example of the lifetime anomalies first discussed by Douglas.[19] That is, mixing of the rovibronic levels in the SiH_2 $\tilde{A}\,^1B_1$ state with background levels (either of the $\tilde{a}\,^3B_1$ or high vibrational levels of the $\tilde{X}\,^1A_1$) leads to perturbation both in the energy levels, with the ensuing complications in assigning the spectrum, and in the oscillator strength associated with each level. Such lifetime variations have been observed in diatomics[16,20–22] and in polyatomic molecules,[23–29] but the range of variation found in this system is comparable only to that of the fluorescence decay rates found in the S_1 ($\tilde{A}\,^1A_2$) state of formaldehyde.[24–26]

In order to assess the nature of the interaction leading to these lifetime variations, it would be very helpful to have an estimate of the unperturbed pure radiative lifetime τ°_{rad}. Such an estimate can be obtained from absorption data using standard relationships.[30] Jasinski[12] has measured absorbance on several lines in the $\tilde{A}\,^1B_1(020)$–$\tilde{X}\,^1A_1(000)$ band of SiH_2, using the laser resonance absorption flash kinetic spectroscopy technique. He estimates 10% absorption for the ${}^RQ_{0,J}(5)$ line at 17 259.44 cm^{-1}. Using standard expressions for the rotational partition function,[31] assuming a temperature of 300 K, and other parameters from Ref. 12, we estimate an absorption coefficient $k_\nu = 5.9\times10^{-4}$ cm^{-1} and $\tau^\circ_{rad} = 36\,\mu s$ *if* the yield of SiH_2 in the dissociation is 100%. Since we have estimated that the actual SiH_2 yield in UV photolysis of ϕSiH_3 is on the order of 1%, and the resulting value of τ°_{rad} scales with SiH_2 density, this gives us an estimate of $\sim0.3\,\mu s$ for the unperturbed SiH_2 $\tilde{A}\,^1B_1$ lifetime. Obi and Mayama[9(b)] find a radiative decay rate of $(1.3\pm0.2)\times10^6$ s^{-1} for the rotationless (020) level in supersonically cooled SiH_2, which agrees reasonably well with our measurement of 0.89 μs for the $J=0, K_a=0$ level [Fig. 1(b)], but is somewhat longer than our rough estimate from the absorbance data. For the analogous $\tilde{b}\,^1B_1$–$\tilde{a}\,^1A_1$ transition in CH_2, lifetimes in the range 1.3–4.2 μs have been measured[32–34] albeit without the degree of level-to-level variation observed in this system. Gordon and co-workers[35] have recently carried out *ab initio* calculations on the SiH_2 $\tilde{X}\,^1A_1$, $\tilde{a}\,^3B_1$, and $\tilde{A}\,^1B_1$ states; from their calculated $\tilde{A}$–$\tilde{X}$ oscillator strengths, we estimate $\tau^\circ_{rad} = 0.15\,\mu s$ for the (020) level, which is consistent with the value estimated from the absorption[12] or supersonic beam[9(b)] data.

Before proceeding with a description of our proposed model, which incidentally bears both similarities with and differences from the currently accepted model relating to the decay mechanisms for S_1 formaldehyde,[24–26] it will be instructive to further examine the decay data for SiH_2 $\tilde{A}(020)$.

As can be seen from Fig. 2, the majority of measured lifetimes for *assigned* transitions in the (020)–(000) band lie below the estimated value of τ°_{rad}. However, there are a few lifetimes that are considerably longer than the estimated value of τ°_{rad}. Careful inspection of the data leads us to conclude that there are few correlations between the magnitudes of the observed lifetimes and the rotational quantum numbers of the emitting states. Very short lifetimes ($\lesssim20$ ns) are observed for a variety of states with low J,K_a quantum numbers, for states with high J,K_a quantum numbers and for states with high J, low K_a quantum numbers. For example, the three longest-lived states (in the assigned data set) correspond to the levels $J=5, K_a=2$ (678 ns), $J=2, K_a=1$ (738 ns) and $J=0, K_a=0$, blended with $J=1, K_a=1$ [27 and 898 ns; see Fig. 1(b)].[36] By way of comparison, two examples of short-lived states are $J=4$, $K_a=1$ (9 ns) and $J=2$, $K_a=1$ ($\lesssim7$ ns).

The set of assigned lines for the (020)–(000) band accounts for most of the allowed transitions terminating in $\tilde{A}$ rovibronic states with J up to about 5. Few of the assigned lines refer to transitions terminating in states with $5\leqslant J\leqslant10$ (thermal population falls off for $J''\gtrsim8$). Hence it is highly probable that many of the unassigned (and therefore presumably more perturbed) lines correspond to transitions involving higher J values. These observations might be interpreted as suggesting that the higher J states couple more strongly with the perturbing manifold, a suggestion that is consistent with the $\sim J^2$ dependence of rovibronic coupling matrix elements.[37]

The model we propose to explain the wide level-to-level variation in the fluorescence decay of SiH_2 ($\tilde{A}\,^1B_1$) is arrived at through a process of elimination. Zero-order rovibronic levels of the $\tilde{A}\,^1B_1$ state of SiH_2, defined by the quantum numbers $(v_1,v_2,v_3,J,K_a,K_c,M_J)$ are eigenfunctions of a near-prolate ($\kappa=-0.873$) asymmetric rotor Hamiltonian.[10] In the $\tilde{A}\,^1B_1$ state, SiH_2 is bent at an angle of 123° in its equilibrium position. These zero order levels are embedded in the zero order levels of the ground singlet $\tilde{X}\,^1A_1$ state (equilibrium H–Si–H angle of 92.1°, near oblate asymmetric rotor with $\kappa=+0.511$)[10] and the first excited triplet state $\tilde{a}\,^3B_1$ (equilibrium H–Si–H angle of 118.1° calculated *ab initio*,[35,38] near prolate asymmetric rotor[39] with $\kappa=-0.78$).

For discussion, we focus attention on the $\tilde{A}(020)$ rovibronic manifold. The (020), $J=0$ level lies 17 248 cm^{-1} above the $\tilde{X}(000)$, $J=0$ state.[10] The $\tilde{a}\,^3B_1$–$\tilde{X}\,^1A_1$ splitting has been estimated as ~18 kcal $mol^{-1} = 6300$ cm^{-1} on the basis of *ab initio* calculations[35] and photoionization mass spectrometry.[40] This would place the $\tilde{A}\,^1B_1$ (020) level approximately 10 950 cm^{-1} above $\tilde{a}\,^3B_1(000)$. We propose that zero-order rovibronic levels in the $\tilde{A}(020)$ state are:

(i) mixed through the nuclear kinetic energy operator $\tilde{T}_N$ with zero-order levels $\gamma S_0 = (v_1,v_2,v_3)$ of the $\tilde{X}$ state, with coupling matrix elements

$$\langle\psi^j_S|\tilde{T}_N|\psi^i_S\rangle, \tag{1}$$

where ψ^j_S and ψ^i_S are the zero-order rovibronic wave functions for the $\tilde{X}(\gamma S_0)$ and $\tilde{A}(020)$ states, respectively;

(ii) mixed through the spin–orbit operator $\tilde{\mathscr{H}}_{SO}$ with zero-order levels $\gamma T = (v_1,v_2,v_3)$ of the $\tilde{a}$ triplet state, with coupling matrix elements

$$\langle \psi_T^j | \tilde{\mathscr{H}}_{SO} | \psi_S^i \rangle, \tag{2}$$

where ψ_T^j refers to the zero-order rovibronic wave function for $\tilde{a}(\gamma T)$. Furthermore, the $\tilde{a}$ state and the $\tilde{X}$ state of SiH_2 must also be strongly coupled, as has been shown to be the case in the analogous $\tilde{a}\,^1A_1$–$\tilde{X}\,^3B_1$ system of methylene,[41] with matrix elements analogous to expression (2).

A rough estimate of the pure vibronic density of states shows immediately that the density of background levels is insufficient to account for the observed variation in the lifetimes. The density in S_0 is approximately 0.05 per cm^{-1}, and in T_1 approximately 0.02 per cm^{-1}, at an excitation energy of 17 000 cm^{-1} above the S_0 origin. We are thus led to consider the full rovibronic density of states. In doing so, one must be wary of the strict constraints on changes in angular momentum quantum numbers that normally inhibit widespread coupling between rovibronic manifolds.[37] For S_1–S_0 coupling in SiH_2, the matrix elements given by expression (1) are expected to conform to the usual selection rules on J and M, i.e., that $\Delta J = 0$ and $\Delta M = 0$. We propose however that the $\Delta K = 0$ restraint may no longer apply. Although the large geometry change in going from S_1 to S_0 is not itself a sufficient condition for K breakdown,[42] other mechanisms exist at moderate to high excitation for relaxation of $\Delta K = 0$.

The relaxation of the ΔK selection rule has important ramifications, as we shall discuss below.

S_1–T_1 coupling will follow more closely the restrictions that normally apply in the symmetric rotor case,[37] i.e., the nonvanishing matrix elements arising from expression (2) will be those for which $\Delta N = 0, \pm 1$ and $\Delta K = 0, \pm 1$, where the coupling of electron spin and rotational angular momentum is given by the vector sum $\mathbf{J} = \mathbf{S} + \mathbf{N}$. The close adherence to these selection rules follows since the geometry of the triplet state is similar to that of the first excited singlet state of SiH_2. Of course, there will be a small degree of relaxation of the $\Delta K = 0, \pm 1$ restriction due to asymmetry, and due to the fact that the asymmetry parameter is slightly different in the S_1 and T_1 states. On the other hand, T_1–S_0 coupling in SiH_2 should show the same drastic relaxation of the $\Delta K = 0, \pm 1$ selection rules.

The consequences of the relaxation of the ΔK selection rule are as follows:

(i) Rovibronic levels $|020;J,K\rangle$ in $\tilde{A}$ will couple extensively with all $|\gamma S;J,K'\rangle$ levels (same symmetry, same J, any K) in $\tilde{X}$ that lie within an appropriately close energy interval. Note that the K stacks in $\tilde{X}$ (near oblate) descend with increasing K, while the K stacks in $\tilde{A}$ (near prolate) ascend with increasing K. Hence the number of rovibronic levels in $\tilde{X}$, with appropriate symmetry and the same J, that will be in near resonance with a given $|020;J,K\rangle$ level, will be much larger than if SiH_2 were either near oblate or near prolate in both states.

We have carried out model calculations to establish this point. The S_0 vibrational level structure in the vicinity of $\tilde{A}(020)$ is estimated using known vibrational frequencies,[10,43] and known or estimated anharmonicities.[43] Rotational stacks are built explicitly on each of the vibrational levels and hence we may determine the number of S_0 levels that lie within a span of a few cm^{-1} of each $S_1|020;J,K\rangle$ state. A typical model calculation is illustrated in Fig. 5. We see that when the $\Delta K = 0$ restriction is relaxed, the number of $S_0|\gamma_S;J,K\rangle$ levels lying within a $\pm$ 10 cm^{-1} range of a specific $S_1|020;J,K\rangle$ state increases substantially, e.g., in the case of $|J = 7, K = 2\rangle$, we find no S_0 level within $\pm$ 10 cm^{-1} under the $\Delta K = 0$ restriction, but lifting the $\Delta K = 0$ restriction provides $\sim$ 10 accessible S_0 levels. (Note that for methylene,[41] $\tilde{a}$–$\tilde{X}$ coupling matrix elements are found to be on the order of 6 cm^{-1}.)

(ii) Similar calculations show that T_1–S_0 coupling will be widespread in the vicinity of the $\tilde{A}(020)$ rotational manifold. In contrast, direct S_1–T_1 coupling will be sporadically distributed since the $\Delta K = 0, \pm 1$ restriction will hold reasonably well. However, since T_1 and S_0 are extensively mixed with each other in the vicinity of $S_1(020)$, and since S_1 and S_0 are likewise extensively mixed, we may suppose that the eigenfunction of most of the "$S_1(020)$" levels will be admix-

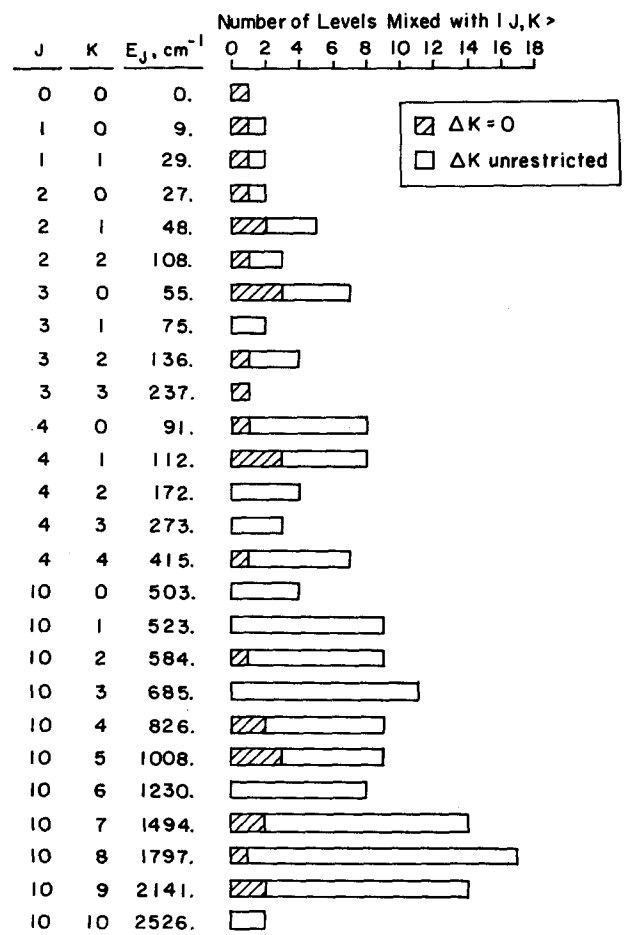

FIG. 5. Model calculations for the number of $\tilde{X}\,^1A_1$ levels lying within $\pm$ 10 cm^{-1} of specific $|\tilde{A}\,^1B_1,020,J,K\rangle$ levels of SiH_2. Measured vibrational and rotational constants (Ref. 10) and anharmonicities (Ref. 43) are used to estimate the $\tilde{X}\,^1A_1$ level structure in the vicinity of $\tilde{A}\,^1B_1$ (020). Calculations are shown for both low-J (0,1,2,3,4) and high-J(10) zero-order rovibronic levels of $\tilde{A}\,^1A_1(020)$.

tures of substantial but varied fractions of the zero-order states of S_1, T_1, and S_0.

We now connect the picture of rovibronic coupling that we have developed thus far, for the $SiH_2\,\tilde{A}(020)$ state embedded in the nearby manifolds of the $\tilde{a}\,^3B_1$ and $\tilde{X}\,^1A_1$ states, with the observed wide variations in fluorescence lifetime.

We estimated previously that the pure radiative lifetime τ°_{rad} of the $\tilde{A}$ electronic state is approximately 0.3 μs. Observed fluorescence lifetimes are found to be both substantially *shorter* and substantially *longer* than τ°_{rad}. The longer lifetimes may be attributed, in principle, to a substantial fraction of triplet ($\tilde{a}\,^3B_1$) or ground state singlet ($\tilde{X}\,^1A_1$) character in the emitting $\tilde{A}(020;J,K)$ state. Lifetime shortening, on the other hand, can only occur in the present context if a nonradiative channel competes with spontaneous emission.

As may be seen from the model calculations presented in Fig. 5, there is nowhere near sufficient density of S_0 levels, even with complete relaxation of the restriction on ΔK, to provide a statistical-case, or even intermediate-case radiationless decay channel. Our observation of single exponential decays confirms our proposition, which arises therefrom, that the fast decay times are *not* a consequence of dephasing following coherent excitation of a bunch of close-lying stationary states.

We are thus led to the proposition that the nonradiative channel that manifests itself as lifetime shortening of the $\tilde{A}$ state is molecular predissociation, as has also been suggested by Obi.[9(b)] A schematic diagram showing the relevant details of the energetics for SiH_2 dissociation to Si + H_2 is shown in Fig. 6. The heat of formation of ground-state SiH_2 is estimated[11,40,44] to be $\sim$66 kcal mol^{-1} above the reference state; the $\tilde{a}\,^3B_1$ state is estimated[35,38,40] to lie at an energy of 6330 cm^{-1} (18 kcal mol^{-1}) above S_0, and the origin[10] of the $\tilde{A}\,^1B_1$ level is at 15 990 cm^{-1} (45.7 kcal mol^{-1}) above S_0. The heat of vaporization of Si(s) is $\sim$105 kcal mol^{-1} [45]; therefore Si(g) + H_2 (g) lies 6 to 7 kcal mol^{-1} above the $\tilde{A}\,^1B_1$ origin. This is also consistent with the bond dissociation energy of SiH ($D^\circ_0 \leqslant 3.06$ eV = 70.5 kcal mol^{-1}).[17,40] The ground electronic state of Si is ^3P, however, and the SiH_2 singlet surfaces correlate with Si(^1S,^1D) states which lie at higher energies than the prepared SiH_2 levels.[11] Since the Si(^3P) + H_2 surface correlates directly with that for $SiH_2\,\tilde{a}\,^3B_1$, the barrier to elimination of H_2 should be low for the $\tilde{a}\,^3B_1$ manifold. Fredin *et al.*[43] have suggested, on the basis of the Si + H_2 reaction in low-temperature matrices, that there is in fact no barrier along this reaction coordinate. Recall that the lifetimes of rovibronic levels of $\tilde{b}\,^1B_1$ CH_2, measured by ourselves and the other workers,[32–34] are of the order of several μs and do not show marked level-to-level variation. Since the $\tilde{b}\,^1B_1$ state lies $\sim$50 kcal mol^{-1} *below* the first C + H_2 dissociation channel, the coupling to a dissociation continuum is not possible for this state of CH_2, and thus no lifetime shortening occurs.

We see that there are two ingredients necessary for efficient molecular predissociation from the $\tilde{A}\,^1B_1$ state of SiH_2. First, the rovibronic level in $\tilde{A}\,^1B_1$ must be coupled substantially to a rovibronic level of $\tilde{a}\,^3B_1$. Second, that triplet level must be coupled to the dissociation channel. As we have argued above, S_1 and T_1 are likely to be mixed only sporadically. However, S_1 and S_0, as well as T_1 and S_0 are likely to be

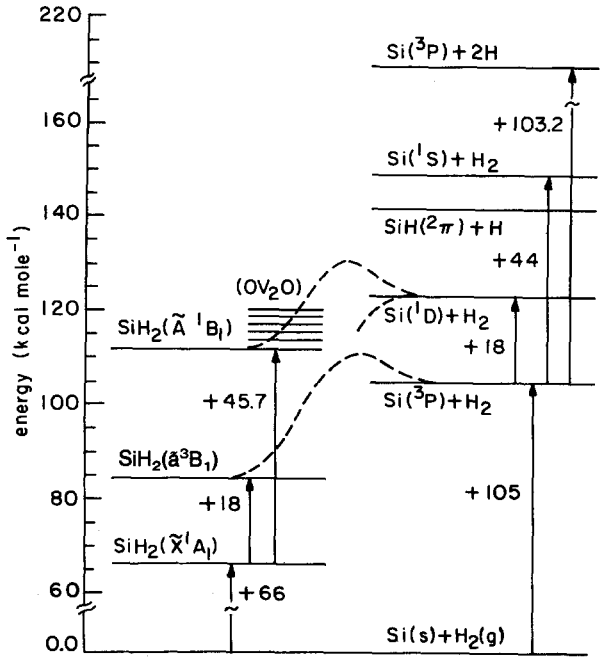

FIG. 6. Schematic of the energetics relating to SiH_2 molecular predissociation. Energies are in kcal mol^{-1} (see the text for details). The dashed lines connecting the $SiH_2\,\tilde{a}\,^3B_1$ and $\tilde{A}\,^1B_1$ levels with the Si(*g*) + H_2(*g*) level are meant to be merely suggestive of the possible potential barriers.

extensively mixed. Our model calculations show that the mixing is not ordered in any obvious form, but rather it depends on the quasirandom spacings of S_0 and T_1 levels in the vicinity of the $\tilde{A}$ state. Accordingly, the lifetime shortening, a consequence of the *squared* fraction of dissociative triplet that is mixed with the S_1 zero-order state, will vary dramatically.

The question now arises as to why there are some rovibronic states which possess a fluorescence lifetime which may be significantly longer than the estimated τ°_{rad}. Perhaps the simplest explanation is that these states are mixed most strongly with the ground electronic state (S_0), which cannot readily dissociate to Si(^3P) + H_2. If τ°_{rad} were actually much longer than our estimate ($\sim$0.3 μs), then this issue would not arise, since all the observed fluorescence lifetimes would have been reduced from τ°_{rad}, by the predissociation mechanism we have proposed. This is quite unlikely to be the case, however, on the basis of both the absorption experiment[12] and theoretical calculations.[35]

V. DISCUSSION

The rovibronic levels of $SiH_2\,\tilde{A}\,^1B_1$ are strongly perturbed by mixing with background levels of $\tilde{X}\,^1A_1$ and $\tilde{a}\,^3B_1$. This is manifested as irregularities in both line positions (over half the observed lines are unassigned and cannot be fit with a standard rotational Hamiltonian) and wide variations of fluorescence lifetimes of individual levels. The decrease in fluorescence lifetimes, as compared with the expected pure ra-

diative lifetime, is attributed to predissociation to $Si(^3P) + H_2$. Silicon atoms have been detected by resonance fluorescence in rf discharges in silane,[46,47] and predissociation of electronically excited SiH_2 may be one of the processes leading to atomic Si formation in such systems. We also note that SiH_2 is formed in high yield in the IRMPD of alkylsilanes, even though it is not a product of the initial decomposition step; it is formed in much lower yield in the UV photolysis of phenylsilane.

Our model of the predissociation mechanism involves a number of background states coupling with each rovibronic level of $\tilde{A}\,^1B_1$. Since the spectroscopic parameters for the $\tilde{X}\,^1A_1$ state are not known at these energies, and those for the $\tilde{a}\,^3B_1$ state are not known at all experimentally, it is not possible to calculate lifetimes for specific levels. Some recently developed algebraic techniques[48–50] for finding a distribution of level spacings in polyatomic molecules may prove useful in estimating a distribution of detunings, and therefore of lifetimes, for a set of levels in such a perturbed molecule. Engel *et al.*[51] have applied a maximal-entropy procedure directly to the lifetime data presented here, and have found that the distribution of lifetimes (and presumably of the associated level spacings) is fully chaotic.

The wide variation in lifetimes from one level to the next means that extreme care must be taken in determining, e.g., electronic quenching cross sections, since non-Stern–Volmer behavior will result if excitation bandwidths are insufficiently narrow to excite only a single rovibronic level.[25] Similar precautions should be exercised when using LIF detection to carry out kinetic measurements on SiH_2.

ACKNOWLEDGMENTS

We would like to thank the Laser Research Facility at the G.R. Harrison Spectroscopy Laboratory for the loan of the transient digitizer, Dr. P. Vaccaro for providing several computer programs, Drs. J. Jasinski, M. Gordon, D. Rayner, J.S. Francisco, and S. Kable for unpublished data and helpful discussions, and the referee for insightful comments. This research was supported by Air Force Office of Scientific Research Contract F19628-86-C-0139, by the U.S.–Australian Cooperative Science Program, N.S.F. Grant INT84-12215, and by the Australian Research Grants Scheme Grant C79-15129.

[1]B. A. Scott, R. M. Plecenik, and E. E. Simonyi, Appl. Phys. Lett. **39**, 73 (1981).
[2]B. A. Scott, M. H. Brodsky, D. C. Green, D. B. Kirby, R. M. Plecenik, and E. E. Simonyi, Appl. Phys. Lett. **37**, 725 (1980).
[3]J. W. Erwin, M. A. Ring, and H. E. O'Neal, Int. J. Chem. Kinet. **17**, 1067 (1985).
[4]T. F. Deutsch, J. Chem. Phys. **70**, 1187 (1979).
[5]P. A. Longeway and F. W. Lampe, J. Phys. Chem. **87**, 354 (1983).
[6]J. S. Francisco, S. Joyce, J. I. Steinfeld, and F. Walsh, J. Phys. Chem. **88**, 3098 (1984).
[7]J. W. Thoman, Jr. and J. I. Steinfeld, Chem. Phys. Lett. **124**, 35 (1986).
[8]D. M. Rayner, R. P. Steer, P. A. Hackett, C. Wilson, and P. John, Chem. Phys. Lett. **123**, 449 (1986).
[9](a) G. Inoue and M. Suzuki, Chem. Phys. Lett. **105**, 641 (1984); (b) K. Obi and S. Mayama, Abstract I-12, Int. Symp. Gas Kinet. (Bordeaux, France, July 1986).
[10]I. Dubois, Can. J. Phys. **46**, 2485 (1968).
[11]J. S. Francisco (private communication).
[12]J.M. Jasinski, J. Phys. Chem. **90**, 555 (1986).
[13]C. D. Eley, M. C. A. Rowe, and R. Walsh, Chem. Phys. Lett. **126**, 153 (1986).
[14]G. Inoue and M. Suzuki, Chem. Phys. Lett. **122**, 361 (1985).
[15]A. E. W. Knight, B. K. Selinger, and I. G. Ross, Aust. J. Chem. **26**, 1159 (1973); A. E. W. Knight and B. K. Selinger, *ibid.* **26**, 1, 499 (1973).
[16]R. W. Field, O. Benoist d'Azy, M. Lavollée, R. Lopez-Delgado, and A. Tramer, J. Chem. Phys. **78**, 2838 (1983).
[17]G. Herzberg and J.W.C. Johns, Proc. R. Soc. London Ser. A **295**, 107 (1966).
[18]K. P. Huber and G. Herzberg, *Molecular Spectra and Molecular Structure. IV. Constants of Diatomic Molecules* (Van Nostrand Reinhold, New York, 1979), p. 598
[19]A. E. Douglas, J. Chem. Phys. **45**, 1007 (1966).
[20]M. Broyer, J. Vigue, and J.-C. Lehmann, J. Chem. Phys. **64**, 4793 (1976).
[21]Y. Matsumi, T. Suzuki, T. Munakata, and T. Kasuya, J. Chem. Phys. **83**, 3798 (1985).
[22]A. J. Hynes and J. H. Brophy, Chem. Phys. Lett. **63**, 93 (1983).
[23]F. Shimizu and K. Shimizu, J. Chem. Phys. **78**, 2798 (1983).
[24]J. C. Weisshaar and C. B. Moore, J. Chem. Phys. **72**, 5415 (1980).
[25]J. C. Weisshaar, Ph.D. thesis, University of California, Berkeley (1974).
[26]D. R. Guyer, W. F. Polik, and C. B. Moore, J. Chem. Phys. **84**, 6519 (1986).
[27]K. Shibuya, P. W. Fairchild, and E. K. C. Lee, J. Chem. Phys. **75**, 3397 (1981).
[28]U. Schubert, E. Riedle, and H. J. Neusser, J. Chem. Phys. **84**, 5326 (1986).
[29]U. Schubert, E. Riedle, H. J. Neusser, and E. W. Schlag, J. Chem. Phys. **84**, 6182 (1986).
[30]J. I. Steinfeld, *Molecules and Radiation*, 2nd ed. (M.I.T., Cambridge, Mass., 1985), pp. 25–31.
[31]D. McQuarrie, *Statistical Mechanics* (University Science Books, Mill Valley, CA, 1976), p. 136.
[32]G. R. Mohlmann and F. J. De Heer, Chem. Phys. Lett. **43**, 236 (1976).
[33]J. Danon, S. V. Filseth, D. Feldmann, H. Zacharias, C. H. Dugan, and K. H. Welge, Chem. Phys. **29**, 345(1978).
[34]A. J. Grimley and J. C. Stephenson, J. Chem. Phys. **74**, 447 (1981).
[35]S. Koseki and M. S. Gordon, J. Mol. Spectrosc. (submitted).
[36]On the basis of the measured [Ref. 9(b)] radiative rate for the rotationless (020) level, we assign the long (898) ns component of the biexponential decay to 0_{00}, and the remaining short (27 ns) to 1_{10}.
[37]W. E. Howard and E. W. Schlag, in *Radiationless Transitions*, edited by S. H. Lin (Academic, New York, 1980), p. 81; E. K. C. Lee and G. L. Loper, *ibid.*, p. 2.
[38]M. E. Colvin, R. S. Grev, H. F. Schaefer III, and J. Bicerano, Chem. Phys. Lett. **99**, 399 (1983).
[39]Rotational constants for SiH_2 $\tilde{a}\,^3B_1$ have been calculated by us using the geometry determined *ab initio* in Ref. 38, viz.: $A = 15.77\ cm^{-1}$, $B = 5.29\ cm^{-1}$, $C = 3.97\ cm^{-1}$.
[40]J. Berkowitz, J. P. Greene, H. Cho, and B. Ruščić, J. Chem. Phys. **86**, 1235 (1987).
[41]H. Petek, D. J. Nesbitt, D. C. Darwin, and C. B. Moore, J. Chem. Phys. **86**, 1172 (1987); H. Petek, D. J. Nesbitt, C. B. Moore, F. W. Birss, and D. A. Ramsay, *ibid.* **86**, 1189 (1987).
[42](a) E. J. Heller, J. Chem. Phys. **68**, 2066 (1978); (b) **72**, 1337 (1980); (c) M. Blanco and E. J. Heller, *ibid.* **78**, 2504 (1983); (d) E. J. Heller and R. L. Sundberg, in *Chaotic Behavior in Quantum Systems*, edited by G. Casati (Plenum, New York, 1985), p. 255.
[43]L. Fredin, R. H. Hauge, Z. H. Kafafi, and J. L. Margrave, J. Chem. Phys. **82**, 3542 (1985).
[44]P. John and J.H. Purnell, J. Chem. Soc. Faraday Trans. 1 **69**, 1455 (1973).
[45]*JANAF Thermochemical Tables*, Natl. Bur. Stand. (U.S. GPO, Washington, D.C., 1965).
[46]R. M. Roth, K. G. Spears, and G. Wong, Appl. Phys. Lett. **45**, 28 (1984).
[47]K. G. Spears, T. J. Robinson, and R. M. Roth, IEEE Trans. Plasma Sci. **PS-14**, 179 (1986).

[48]V. Buch, R. B. Gerber, and M. A. Ratner, J. Chem. Phys. **76**, 5397 (1982).
[49]O. S. van Roosmalen, F. Iachello, R. D. Levine, and A. E. L. Dieperink, J. Chem. Phys. **79**, 2515 (1983).
[50]I. Benjamin, V. Buch, R. B. Gerber, and R. D. Levine, Chem. Phys. Lett. **107**, 515 (1984).
[51]Y. M. Engel, R. D. Levine, J. W. Thoman, Jr., J. I. Steinfeld, and R. I. McKay, J. Chem Phys. **86**, xxxx (1987).